Filomat 35:13 (2021), 4305–4326
https://doi.org/10.2298/FIL2113305A

Published by Faculty of Sciences and Mathematics,
University of Niš, Serbia
Available at: http://www.pmf.ni.ac.rs/filomat

Generalized Hyperbolic Secant Distribution: Properties, Estimation, and Applications

Mohammad A. Aljarrah[a]

[a] *Department of Mathematics, Tafila Technical University, 66110 Tafila, Jordan*

Abstract. In this study, we define a generalized hyperbolic secant distribution. Poor fit to heavy tailed data sets is repeatedly obtained by existing three-parameter distributions. Only three parameters are considered in the proposed new distribution and it fits a heavy left- and right-tailed data better than various existing distributions. We study some properties of the new distribution, namely, mode, skewness, kurtosis, hazard function, moments, mean deviation, and Shannon entropy. Seven different frequentist methods for estimating the parameters are briefly described. A simulation study is also conducted to compare the performances of the proposed methods of estimation. The usefulness of the new model is demonstrated by applying it to fit two real-life data.

1. Introduction

Probability distributions are important in exploring and modeling real-life data in many fields. Thus, this area has been widely examined by many researchers in recent years. The hyperbolic secant (HS) distribution was provided and studied by Talacko [26]. A special case of a class of distributions introduced by Perks [23] was also obtained. Formally, the HS random variable is arising naturally as the logarithm of ratio of two independent standard normal random variables. Specifically, we suppose X_1 and X_2 have two independent standard normal distributions. Then, $Y = \ln(X_1/X_2)$ has an HS distribution. The probability density function (PDF) of a HS distribution is given by

$$f_{HS}(x) = \frac{1}{\pi}\operatorname{sech}(x),\ x \in (-\infty, \infty),$$

and the corresponding cumulative distribution function (CDF) is

$$F_{HS}(x) = \frac{2}{\pi}\tan^{-1}\left(\exp(x)\right),\ x \in (-\infty, \infty),$$

where scale and location parameters can be added using the transformation $Y = \mu + \sigma X$. The HS distribution is similar to a normal distribution. However, it is symmetric with variance equal $(\pi/2)^2$. The HS distribution is also leptokurtic; that is, it has a higher peak and heavier tails than the standard normal distribution.

2020 *Mathematics Subject Classification*. Primary 62E15; Secondary 62F10, 62P35
Keywords. beta-family, hazard function, symmetric distribution, moments
Received: 29 October 2020; Revised: 10 January 2021; Accepted: 27 January 2021
Communicated by Biljana Popović
Email address: aljarrah@ymail.com (Mohammad A. Aljarrah)

Therefore, the normal is reasonably replaced by the HS distribution in some cases. In literature, the fit of the HS distributions has been explored by proposing many generalizations of the HS. These generalized distributions are indexed by one or more shape parameters. They are established to extend the HS model to asymmetric probability density curves and improve the fit in the skewed probability areas. Fischer [13] and the references therein presented a brief contribution on possible generalizations of HS distribution. In this study, a generalized HS (GHS) distribution is introduced by adding one extra shape parameter. The extra parameter adds skewness for HS distribution and control the degree of skewness. Section 2 defines the GHS distribution. We study some properties of the GHS distribution, namely, the shapes of the PDF, hazard rate function (HRF), and quantile function. Section 3 investigates the mode, existence, and expression for the moments. The relationship among the mean, variance, skewness, kurtosis, and the shape parameter is also examined. Shannon's entropy, mean deviation, and order statistics are studied in Section 4. Seven different frequentist methods for estimating the parameters are briefly described in Section 5. A simulation study is also performed to compare the performance of these estimation methods for the presented model. In Section 6, the flexibility and usefulness of the new distribution are demonstrated by applications to two real data sets. Summary and conclusions are elaborated in Section 7.

2. GHS Distribution

The T-X framework was proposed by Alzaatreh et al. [5], and it was further expanded by Aljarrah et al. [4]. The two general methods have been applied to obtain various generalization of distributions. Recently, Aljarrah et al. [3] defined the exponential-normal{Generalized Weibull} (E-N{GW}) distribution as a generalization of the normal distribution. The authors also explored various properties of this model. Following the technique by Aljarrah et al. [3], we define the T-HS{GW} generalized family as follows: Given a shape parameter $\xi > 0$, location parameter $-\infty < \mu < \infty$, and scale reflection parameter $\sigma \neq 0$, we define the generalized family of distribution T-HS{GW} as

$$F_X(x) = \frac{1}{2} - sgn(\sigma)\left(\frac{1}{2} - F_T\left\{\left[\left(1 - \tfrac{2}{\pi}\tan^{-1}\left(\exp\left(\tfrac{x-\mu}{\sigma}\right)\right)\right)^{-\xi} - 1\right]/\xi\right\}\right), \tag{2.1}$$

where $sgn(\sigma)$ is the sign of the parameter σ. and F_T is the CDF of a random variable $T \in (0, \infty)$. The corresponding PDF to (2.1) is given by

$$f_X(x) = \frac{2\exp\left(\frac{x-\mu}{\sigma}\right)\left(1 + \exp\left(2\frac{x-\mu}{\sigma}\right)\right)^{-1}}{\pi|\sigma|\left(1 - \frac{2}{\pi}\tan^{-1}\left(\exp\left(\frac{x-\mu}{\sigma}\right)\right)\right)^{\xi+1}} f_T\left\{\frac{\left(1 - \frac{2}{\pi}\tan^{-1}\left(\exp\left(\frac{x-\mu}{\sigma}\right)\right)\right)^{-\xi} - 1}{\xi}\right\}. \tag{2.2}$$

It is noteworthy to mention the method presented in (2.2) is not to develop a single generalized HS distribution, it can be applied to generate different families of generalized HS distributions. The GHS distribution can be defined from (2.2) by letting T be the exponential random variable as follows:

Definition 2.1. *We respectively define the PDF and CDF of the GHS distribution as*

$$f_X(x) = \frac{2\exp(\frac{x-\mu}{\sigma})\left(1 + \exp(2\frac{x-\mu}{\sigma})\right)^{-1}}{\pi|\sigma|\left(1 - \frac{2}{\pi}\tan^{-1}\left(\exp\left(\frac{x-\mu}{\sigma}\right)\right)\right)^{\xi+1}} \exp\left\{\left[1 - \left(1 - \tfrac{2}{\pi}\tan^{-1}\left(\exp\left(\tfrac{x-\mu}{\sigma}\right)\right)\right)^{-\xi}\right]/\xi\right\}, \tag{2.3}$$

and

$$F_X(x) = \frac{1}{2} - sgn(\sigma)\left(\exp\left\{\left[1 - \left(1 - \tfrac{2}{\pi}\tan^{-1}\left(\exp\left(\tfrac{x-\mu}{\sigma}\right)\right)\right)^{-\xi}\right]/\xi\right\} - \frac{1}{2}\right), \tag{2.4}$$

where, $-\infty < x, \mu < \infty, \sigma \neq 0, \xi > 0.$

Notably, GHS distribution is derived as a generalization of the symmetric HS distribution for fitting highly skewed data. As a result, good comparison of performance can be conducted when comparing with various existing three- and four-parameter distributions.

Corollary 2.2. *When $\xi \to 0$, the PDF of $GHS(\mu, \sigma, \xi)$ distribution in* (2.3) *reduces to HS distribution with location and scale parameters μ and $|\sigma|$.*

Proof. $\lim_{\xi \to 0} f_X(x) = \frac{2\exp\left(\frac{x-\mu}{\sigma}\right)}{\pi|\sigma|\left(\exp\left(2\frac{x-\mu}{\sigma}\right)+1\right)} = \frac{1}{\pi|\sigma|}\operatorname{sech}\left(\frac{x-\mu}{\sigma}\right)$, *that is* $X \sim HSD(\mu, |\sigma|)$. □

Quantile functions can be used to generate pseudo-random numbers from a probability distribution. We set $F_X(Q_X(u)) = u$ in (2.4) and solve for $Q_X(u)$ in terms of u. Thus, the following quantile function for the GHS distribution is obtained:

$$Q_X(u) = \mu + \sigma \ln\left(\tan\left[\frac{\pi}{2}\left\{1 - \left\{1 - \xi \ln\left(\tfrac{1}{2} - sgn(\sigma)(u - \tfrac{1}{2})\right)\right\}^{-1/\xi}\right\}\right]\right),\ u \in (0, 1). \tag{2.5}$$

Proposition 2.3.

(a) If T is a standard exponential random variable, then $X = \mu + \sigma \ln\left(\tan\left\{\frac{\pi}{2}\left(1 - (1 + \xi T)^{-1/\xi}\right)\right\}\right)$ follows the $GHS(\mu, \sigma, \xi)$ distribution in Equation (2.4).

(b) If $X \sim GHS(\mu, \sigma, \xi)$, then $(2\mu - X) \sim GHS(\mu, -\sigma, \xi)$.

Proof. The results in (a) and (b) are obtained using the CDF method. □

The HRF of the GHS distribution is obtained after using the CDF in (2.4) and PDF in (2.3). The HRF is given by

$$h(x) = \begin{cases} \dfrac{2\exp(\frac{x-\mu}{\sigma})\left(1 + \exp(2\frac{x-\mu}{\sigma})\right)^{-1}}{\pi|\sigma|\left(1 - \frac{2}{\pi}\tan^{-1}\left(\exp\left(\frac{x-\mu}{\sigma}\right)\right)\right)^{\xi+1}}, & \sigma > 0, \\ \dfrac{2\exp(\frac{x-\mu}{\sigma})\left(1 + \exp(2\frac{x-\mu}{\sigma})\right)^{-1}\left(1 - \frac{2}{\pi}\tan^{-1}\left(\exp\left(\frac{x-\mu}{\sigma}\right)\right)\right)^{-\xi-1}}{\pi|\sigma|\left\{\exp\left\{\left[\left(1 - \frac{2}{\pi}\tan^{-1}\left(\exp\left(\frac{x-\mu}{\sigma}\right)\right)\right)^{\xi} - 1\right]/\xi\right\} - 1\right\}}, & \sigma < 0. \end{cases} \tag{2.6}$$

The plots of PDFs and HRFs for GHS distribution are shown in Figures 1 and 2. The PDF can be symmetric, positively skewed, or negatively skewed. Meanwhile, increasing or increasing-decreasing shapes are observed for the HRF. As observed from the graphs in Figure 1, the distribution tends to be symmetric as $\xi \to 0$, skewed to the left when $\sigma > 0$, and skewed to the right when $\sigma < 0$. The curve of the PDF is reflected about the line $x = 0$ when the sign of parameter σ is changed. The increase in ξ decreases the mode when $\sigma > 0$ and increases the mode when $\sigma < 0$. As observed from the graphs in Figure 2, the HRF in (2.5) increases when $\sigma > 0$. When $\sigma < 0$, the HRF first shows an S-shape trend (constant-–increase-–constant). Then, it increases first and then decreases.

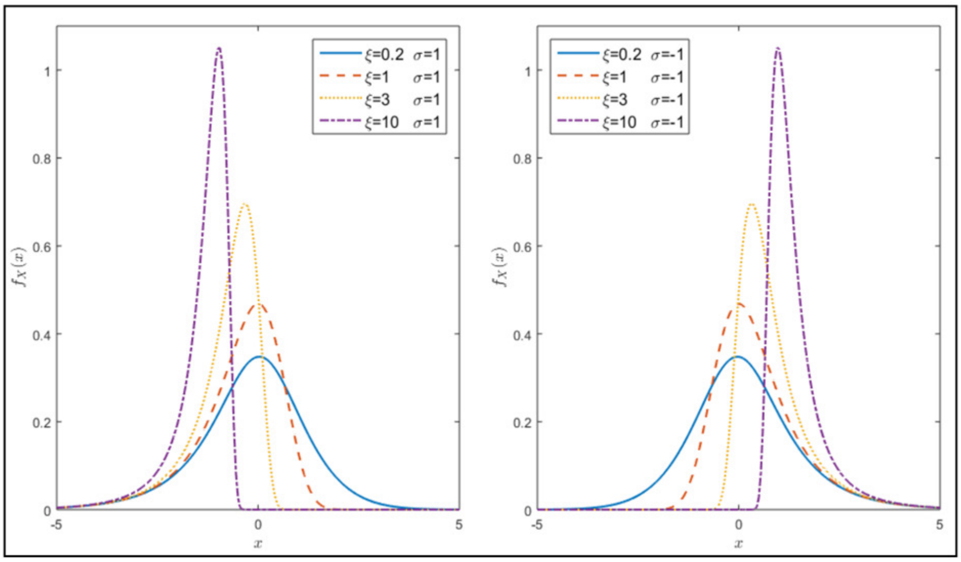

Figure 1: Plots of PDF of GHS distribution with $\mu = 0$.

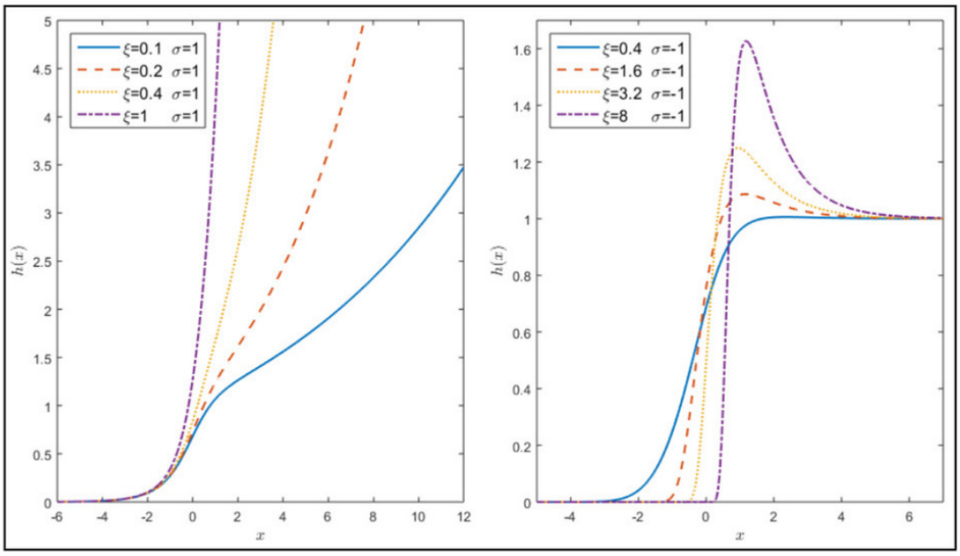

Figure 2: Plots of HRF of GHS distribution with $\mu = 0$.

3. Properties of GHS Distribution

Some properties of the GHS distribution, namely, mode, moments, and relation between the moments and shape parameter ξ, are explored.

3.1. Mode

Theorem 3.1. *The mode of GHS distribution is at the point $x_* = \mu$ when $\xi = \{0, 1\}$. Otherwise, the mode is at the point $x_* = \mu + \sigma \ln(u_*)$, where u_* is the root of the equation*

$$u^{-1}(1-u^2)\left(\pi - 2tan^{-1}(u)\right) - 2\pi^{\xi}\left(\pi - 2tan^{-1}(u)\right)^{-\xi} + 2(\xi+1) = 0, \quad u > 0. \tag{3.1}$$

Proof. *The derivative of $f_X(x)$ in (2.3) is given by*

$$f'_X(x) = f_X(x)\left[\exp\left(\frac{2(x-\mu)}{\sigma}\right)+1\right]^{-1}\left[\pi - 2\tan^{-1}\left(\exp\left(\frac{x-\mu}{\sigma}\right)\right)\right]^{-1} w(x),$$

where

$$w(x) = \frac{1-\exp\left(2(x-\mu)/\sigma\right)}{\exp\left((x-\mu)/\sigma\right)}\left[\pi - 2\tan^{-1}\left(\exp\left(\frac{x-\mu}{\sigma}\right)\right)\right] - 2\left[1-\frac{2}{\pi}\tan^{-1}\left(\exp\left(\frac{x-\mu}{\sigma}\right)\right)\right]^{-\xi} + 2(\xi+1).$$

By setting $w(x) = 0$ and replacing $\exp\left(\frac{x-\mu}{\sigma}\right)$ by u, (3.1) is obtained. Clearly, if $\xi = \{0, 1\}$, then the mode is at $u = 1$ from (3.1); equivalently, $x = \mu$. When $\xi \neq \{0, 1\}$, the mode is at the point $x_* = \mu + \sigma \ln(u_*)$, where u_* is the root of (3.1). □

3.2. Moments

The moments can be used to describe and identify distribution properties, such as the center, standard deviation, skewness, and kurtosis.

Theorem 3.2. *The r^{th} absolute moment of the GHS distribution exists for any $\mu, \sigma \neq 0, \xi > 0$ and satisfies the inequality*

$$E(|X|^r) \leq e^{-1}(1+\xi)^{1+1/\xi}\sum_{i=0}^{r}\binom{r}{i}|\mu|^{n-i}|\sigma|^i E(|R|^i), \tag{3.2}$$

where $E(|R|^r) = \frac{4}{\pi}\Gamma(r+1)\sum\limits_{j=0}^{\infty}(-1)^j(2j+1)^{-(r+1)}$ is the r^{th} absolute moment of a standard HS random variable (Johnson et al., [18]).

Proof. *If $Z = (X-\mu)/\sigma$ and binomial expansion is used, then we have*

$$E(|X|^r) \leq \sum_{i=0}^{r}\binom{r}{i}|\mu|^{r-i}|\sigma|^i E|Z|^i, \tag{3.3}$$

where Z is GHS random variable with $\mu = 0$ and $\sigma = 1$. By using this definition, we obtain

$$\begin{aligned} E(|Z|^i) &= \int_{-\infty}^{\infty}|z|^i \frac{2\exp(z)(1+\exp(2z))^{-1}}{\pi\left(1-\frac{2}{\pi}\tan^{-1}(\exp(z))\right)^{\xi+1}}\exp\left\{\left[1-\left(1-\tfrac{2}{\pi}\tan^{-1}(\exp(z))\right)^{-\xi}\right]/\xi\right\}dz, \\ &= \frac{2}{\pi}\int_{-\infty}^{\infty}|z|^i\frac{\exp(-z)}{(1+\exp(-2z))}g(z)dz, \end{aligned} \tag{3.4}$$

where

$$g(z) = \left(1-\tfrac{2}{\pi}\tan^{-1}(\exp(z))\right)^{-\xi-1}\exp\left\{\left[1-\left(1-\tfrac{2}{\pi}\tan^{-1}(\exp(z))\right)^{-\xi}\right]/\xi\right\}.$$

By using the elementary calculus, we find that $\sup\limits_{-\infty<z<\infty}\{g(z)\} = e^{-1}(1+\xi)^{1/\xi+1}$. From (3.4), we derive

$$E(|Z|^i) \leq e^{-1}(1+\xi)^{1/\xi+1}E(|R|^i), \tag{3.5}$$

where

$$E(|R|^i) = \frac{2}{\pi}\int_{-\infty}^{\infty} |z|^i \frac{\exp(-z)}{(1+\exp(-2z))}dz,$$

is the i^{th} *absolute moment of standard HS distribution. The result in (3.2) is obtained using (3.5) in (3.3).* □

The following theorem presents moments of GHS as a series expression.

Theorem 3.3. *The* r^{th} *moment,* $E(X^r)$*, of the GHS distribution is given by*

$$E(X^r) = \sum_{n=0}^{r}\sum_{i=0}^{n}\sum_{j=0}^{\infty}\binom{r}{n}\binom{n}{i}\mu^{r-n}\sigma^n(-1)^{n+i}\xi^{-i-1}(\pi/2)^{2j}c_{n-i,j}e^{1/\xi}\Gamma(i+1)E^i_{2j/\xi}(1/\xi), \tag{3.6}$$

where $c_{n,m}$ *is given in (3.11), and* $E^j_s(z) = \frac{1}{\Gamma(j+1)}\int_1^{\infty}(\ln t)^j t^{-s}\exp(-zt)dt$ *is the generalized integro-exponential function by (Milgram, [20]).*

Proof. *If* $Z = (X-\mu)/\sigma$*, then we obtain*

$$E(X^r) = \sum_{n=0}^{r}\binom{r}{n}\mu^{r-n}\sigma^n E(Z^n), \tag{3.7}$$

where Z *is a random variable with PDF in (2.3) with* $\mu = 0$ *and* $\sigma = 1$*. Therefore, the moments of* Z *should be obtained. Using Proposition 2.3(a), we derive*

$$E(Z^n) = E\Big\{\ln\tan\Big(\tfrac{\pi}{2}\Big(1-(1+\xi T)^{-1/\xi}\Big)\Big)\Big\}^n.$$

Notably, $\ln\tan(\frac{\pi}{2}-x) = \ln\cot(x) = -\ln\tan(x)$*. Thus, we obtain*

$$E(Z^n) = (-1)^n E\Big\{\ln\tan\Big(\tfrac{\pi}{2}(1+\xi T)^{-1/\xi}\Big)\Big\}^n, \tag{3.8}$$

We use the following series by Gradshteyn and Ryzhik [17](See 1.518-3):

$$\ln\tan(x) = \ln(x) + \sum_{k=1}^{\infty}\underbrace{\frac{(-1)^{k+1}(2^{2k-1}-1)2^{2k}B_{2k}}{k(2k)!}}_{a_k}x^{2k}, 0 < x < \frac{\pi}{2}. \tag{3.9}$$

Thus, we have

$$\Big\{\ln\tan\Big(\tfrac{\pi}{2}(1+\xi T)^{-1/\xi}\Big)\Big\}^n = \left\{(-1/\xi)\ln(1+\xi T) + \sum_{k=0}^{\infty}a_k\Big(\tfrac{\pi}{2}(1+\xi T)^{-1/\xi}\Big)^{2k}\right\}^n, \tag{3.10}$$

where $a_0 = \ln(\pi/2)$*. Applying binomial series on (3.10) yields*

$$\Big\{\ln\tan\Big(\tfrac{\pi}{2}(1+\xi T)^{-1/\xi}\Big)\Big\}^n = \sum_{i=0}^{n}\binom{n}{i}(-1/\xi)^i(\ln(1+\xi T))^i\left(\sum_{k=0}^{\infty}a_k\Big(\tfrac{\pi}{2}(1+\xi T)^{-1/\xi}\Big)^{2k}\right)^{n-i}.$$

Then, we use a result by Gradshteyn and Ryzhik [17] (See 0.314) to increase a power series to a natural number n:

$$\left(\sum_{k=0}^{\infty} a_k u^k\right)^n = \sum_{k=0}^{\infty} c_{n,k} x^k,$$

where the coefficient $c_{n,k}$ is calculated from the recurrence equation

$$c_{n,0} = a_0^n,\ c_{n,m} = \frac{1}{ma_0}\sum_{k=1}^{m}(kn - m + k)a_k c_{n,m-k},\ m \geq 1. \tag{3.11}$$

Therefore, we derive

$$E\Big\{\ln\tan\left(\tfrac{\pi}{2}(1+\xi T)^{-1/\xi}\right)\Big\}^n = \sum_{i=0}^{n}\sum_{j=0}^{\infty}\binom{n}{i}(-1/\xi)^i c_{n-i,j}\Big(\frac{\pi}{2}\Big)^{2j} E\left\{(\ln(1+\xi T))^i(1+\xi T)^{-2j/\xi}\right\}. \tag{3.12}$$

Then, we obtain $E\left\{(\ln(1+\xi T))^i(1+\xi T)^{-2j/\xi}\right\}$ by writing:

$$E\left\{(\ln(1+\xi T))^i(1+\xi T)^{-2j/\xi}\right\} = \int_0^{\infty}(\ln(1+\xi t))^i(1+\xi t)^{-2j/\xi}\exp(-t)dt. \tag{3.13}$$

If $u = 1 + \xi t$ under the integral in (3.13), then we have

$$\begin{aligned} E\left\{(\ln(1+\xi T))^i(1+\xi T)^{-2j/\xi}\right\} &= \frac{e^{1/\xi}}{\xi}\int_1^{\infty}(\ln u)^i u^{-2j/\xi}\exp(-u/\xi)dt, \\ &= \xi^{-1}e^{1/\xi}\Gamma(i+1)E^i_{2j/\xi}(1/\xi). \end{aligned} \tag{3.14}$$

The result in (3.6) is obtained by substituting (3.14) in (3.12) and then using (3.8) and (3.7). □

Figure 3 plots the mean, median, mode, and standard deviation of GHS distribution in terms of the parameter ξ for $\mu = 0$ and $\sigma = \{1, -1\}$. As shown in Figure 3(a), the mean and median decrease with the increase ξ when $\sigma > 0$. Meanwhile, the mode increases first and then decreases with the increase in ξ, and mean < median < mode. When $\sigma < 0$, the mean and median increase with the increase in ξ. Meanwhile, the mode decreases first and then increases with the increase in ξ, and mean > median > mode. Figure 3(b) shows that the standard deviation decreases with the increase in ξ.

Figure 4 plots the skewness and kurtosis of GHS distribution in terms of the parameters ξ when $\mu = 0$ and $\sigma = \{1, -1\}$. As shown in Figure 4(a), the skewness (γ_1) decreases with the increase in ξ when $\sigma > 0$. Moreover, the GHS distribution is left skewed in this case. When $\sigma < 0$, γ_1 increases with the increase in ξ. The GHS distribution is also right skewed in this case. Figure 4(b) shows that the kurtosis (γ_2) decreases first and then increases with the increase in ξ. The kurtosis is also not affected by σ in this case. The distribution is symmetric as $\xi \to 0$. Notably, the degree of γ_1 of the GHS distribution is measured by ξ. The parameter σ plays two roles, namely, characterizing the scale property and determining left skewness ($\sigma > 0$) or right skewness ($\sigma < 0$).

The flexibility of GHSD is compared with the S-transformed HS (HS-SAS) distribution by Fischer and Herrmann [14], the beta-HS (BHS) distribution by Fischer and Vaughan [15], the Burr type VIII (BVIII) distributions by Burr [8], the generalized logistic (GL) distributions of type I and II by Johnson et al. [18], and the skewed normal (SN) distribution by Azzalini [7]. Table 1 summarizes the ranges of the skewness and kurtosis of these distributions. GHS fits the widest range of skewness and kurtosis, with the exception of HS-SAS that can fit platykurtic distributions.

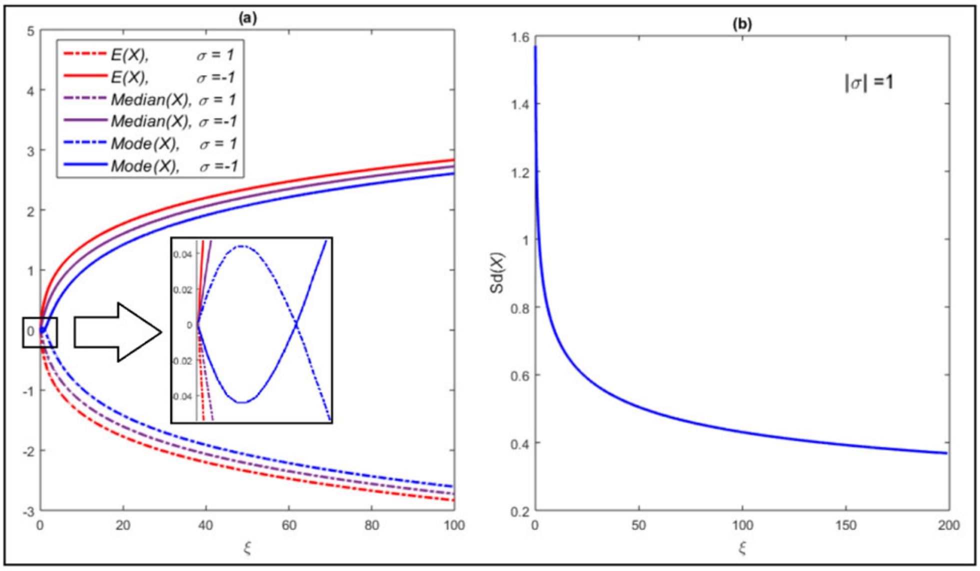

Figure 3: Graphs of mean, median, mode and standard deviation for GHS distribution for $\mu = 0, \sigma = \{1, -1\}$, and various values of ξ.

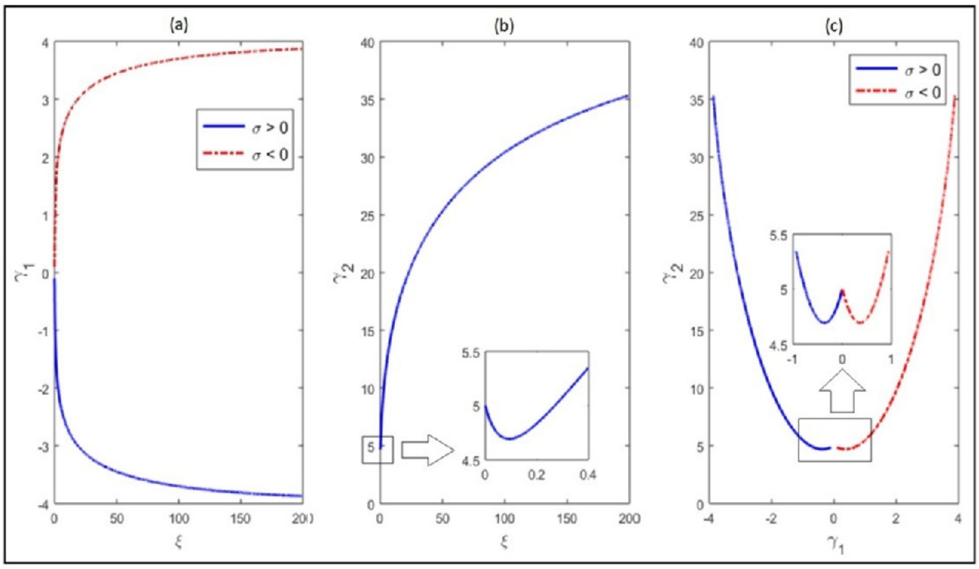

Figure 4: The skewness(γ_1) and kurtosis(γ_2) for GHS distribution for $\mu = 0$ and $\sigma = \{1, -1\}$ for various values of ξ.

Table 1: Comparison of the skewness and kurtosis of GHSD and several competitor distributions

Model	Skewness	Kurtosis
GHS	-3.873 ↔ 3.873	4.696 ↔ 35.033
BHS*	-2.000 ↔ 2.000	3.000 ↔ 9.000
HS-SAS*	-2.900 ↔ 2.900	2.400 ↔ 16.000
BVIII	-1.993 ↔ 1.187	4.940 ↔ 8.971
GLI	-1.995 ↔ 1.134	4.148 ↔ 8.964
GLII	-1.134 ↔ 1.995	4.148 ↔ 8.964
SN	-0.995 ↔ 0.995	3.000 ↔ 3.869

* The kurtosis and skewness are obtained from Figure 6.1 in Fischer [13] (p.56).

4. Shannon's Entropy, Mean Deviations, and Order statistics

4.1. Shannon Entropy

Shannon [24] presented Shannon entropy of any random variable X, which is defined as $H(X) = -E(\ln f_X(x))$. This method provides an absolute limit on the best possible average length of lossless encoding or compression of an information source. We use $f_Y(y) = (1+\xi y)^{-(1+\xi)/\xi}$ and $F_Y(y) = 1-(1+\xi y)^{-1/\xi}$, which are the PDF and CDF of generalized Weibull (Mudholkar et al. [21]), respectively, and combine it with Theorem 2 of Aljarrah et al. [4] to obtain the Shannon entropy of T-$R\{\text{GW}\}$ PDF in (2.2) as follows:

$$H(X) = \ln|\sigma| + H(T) - \tfrac{(1+\xi)}{\xi}E\{\ln(1+\xi T)\} + E\left\{\ln Q'_R\left(1-(1+\xi T)^{-1/\xi}\right)\right\}, \tag{4.1}$$

where T is the standard exponential and R is the HS. The Shannon's entropy (4.1) is obtained by finding $E\left\{\ln Q'_R\left(1-(1+\xi T)^{-1/\xi}\right)\right\}$, where $Q'_R(\lambda) = \pi\csc(\pi\lambda)$ is the derivative of the quantile function of HS distribution. Thus, we obtain

$$\begin{aligned} E\left\{\ln Q'_R\left(1-(1+\xi T)^{-1/\xi}\right)\right\} &= \ln\pi - E\left\{\ln\sin\left[\pi\left(1-(1+\xi T)^{-1/\xi}\right)\right]\right\}, \\ &= \ln\pi - E\left\{\ln\sin\left[\pi(1+\xi T)^{-1/\xi}\right]\right\}. \end{aligned} \tag{4.2}$$

We use the series expansion in Gradshteyn and Ryzhik [17](See 1.518-1),

$$\ln\sin(x) = \ln x + \sum_{k=1}^{\infty}\underbrace{\frac{(-1)^k 2^{2k-1}B_{2k}}{k(2k)!}}_{\omega_k}x^{2k},\ 0 < x < \pi.$$

Thus, we have

$$E\left\{\ln\sin\left[\pi(1+\xi T)^{-1/\xi}\right]\right\} = \ln\pi - \frac{1}{\xi}E(\ln(1+\xi T)) + \sum_{k=1}^{\infty}\omega_k\pi^{2k}E\left((1+\xi T)^{-2k/\xi}\right). \tag{4.3}$$

Thus, we derive the following by using (4.3) in (4.2) and substituting it in (4.1):

$$H(X) = \ln|\sigma| + H(T) - E(\ln(1+\xi T)) - \sum_{k=1}^{\infty}\omega_k\pi^{2k}E\left((1+\xi T)^{-2k/\xi}\right). \tag{4.4}$$

T has standard exponential PDF. Thus, we have

$$H(T) = E\left(-\ln f_T(T)\right) = \int_0^\infty te^{-t}dt = \Gamma(2) = 1. \tag{4.5}$$

Then, we obtain $E\left((1+\xi T)^v\right)$ and $E\left(\ln(1+\xi T)\right)$ by using Formulas (3.382-4) and (4.337) in Gradshteyn and Ryzhik [17]. Therefore,

$$E\left((1+\xi T)^v\right) = \int_0^\infty (1+\xi t)^v \exp(-t)dt = \xi^v e^{1/\xi}\Gamma(1+v, 1/\xi), \tag{4.6}$$

$$E\left(\ln(1+\xi T)\right) = \int_0^\infty \ln(1+\xi t)\exp(-t)dt = e^{1/\xi}E_1(1/\xi). \tag{4.7}$$

where $\Gamma(a,x) = \int_x^\infty t^{a-1}e^{-t}dt$ is the incomplete gamma function, and $E_1(x) = x\int_1^\infty e^{-xt}\ln t\,dt$ is the exponential integral (Abramowitz and Stegun, [2]).

We use (4.7), (4.6), and (4.5) in (4.4) to derive the following Shannon entropy of GHS:

$$H(X) = \ln|\sigma| + 1 - e^{1/\xi}E_1(1/\xi) - \sum_{k=1}^{\infty}\omega_k\pi^{2k}\xi^{-2k/\xi}e^{1/\xi}\Gamma(1-2k/\xi, 1/\xi).$$

4.2. Mean Deviations

X is assumed to be a GHS random variable with mean μ^* and median M^*. The mean deviations from the mean and median are respectively defined as

$$D(\mu^*) = 2\mu^* F_X(\mu^*) - 2I_c(\mu^*) \quad \text{and} \quad D(M^*) = \mu^* - 2I_c(M^*),$$

where F_X is given by (2.4). The mean μ^* can be derived from (3.6) with $r = 1$. The median M^* can be obtained from (2.5) by replacing the value of u with 0.5. After the PDF in (2.3) is used, we obtain the first incomplete moment $I_c(w)$ as

$$I_c(w) = \int_{-\infty}^{w} \frac{2x\exp(\frac{x-\mu}{\sigma})\left(1+\exp(2\frac{x-\mu}{\sigma})\right)^{-1}}{\pi|\sigma|\left(1-\frac{2}{\pi}\tan^{-1}\left(\exp\left(\frac{x-\mu}{\sigma}\right)\right)\right)^{\xi+1}} \exp\left\{\left[1-\left(1-\tfrac{2}{\pi}\tan^{-1}\left(\exp\left(\tfrac{x-\mu}{\sigma}\right)\right)\right)^{-\xi}\right]/\xi\right\}dx.$$

If $t = \left[\left(1-\frac{2}{\pi}\tan^{-1}\left(\exp\left(\frac{x-\mu}{\sigma}\right)\right)\right)^{-\xi} - 1\right]/\xi$, then we have

$$\begin{aligned} I_c(w) &= \int_0^{\left[\left(1-\frac{2}{\pi}\tan^{-1}\left(\exp\left(\frac{w-\mu}{\sigma}\right)\right)\right)^{-\xi}-1\right]/\xi} sgn(\sigma)\left\{\mu + \sigma\ln\tan\left(\frac{\pi}{2}\left[1-(1+\xi t)^{-1/\xi}\right]\right)\right\}\exp(-t)dt, \\ &= sgn(\sigma)\mu F_X(w) + \int_0^{\left[\left(1-\frac{2}{\pi}\tan^{-1}\left(\exp\left(\frac{w-\mu}{\sigma}\right)\right)\right)^{-\xi}-1\right]/\xi} |\sigma|\ln\tan\left(\frac{\pi}{2}\left[1-(1+\xi t)^{-1/\xi}\right]\right)\exp(-t)dt. \end{aligned} \tag{4.8}$$

Notably, $\ln\tan(\frac{\pi}{2}-x) = \ln\cot(x) = -\ln\tan(x)$, and the series in (3.10) is used after setting $n = 1$. Thus, we derive

$$\ln\tan\left(\frac{\pi}{2}\left[1-(1+\xi t)^{-1/\xi}\right]\right) = (1/\xi)\ln(1+\xi T) - \sum_{k=0}^{\infty}\frac{\pi^{2k}}{2^{2k}}a_k(1+\xi T)^{-2k/\xi}. \tag{4.9}$$

Using (4.9) in (4.8) yields

$$I_c(w) = sgn(\sigma)\mu F_T(s) + |\sigma| \left\{ \frac{1}{\xi} \int_0^s \ln(1+\xi T)\exp(-t)dt - \sum_{k=0}^{\infty} \frac{\pi^{2k}}{2^{2k}} a_k \int_0^s (1+\xi T)^{-2k/\xi} \exp(-t)dt \right\}, \tag{4.10}$$

where $s = \left(\left\{ 1 - \frac{2}{\pi}\tan^{-1}\left(\exp\left(\frac{w-\mu}{\sigma}\right)\right)\right\}^{-\xi} - 1 \right)/\xi$. We let $u = 1 + \xi t$ over the integral in (4.10) and use the integral in Gradshteyn and Ryznik [17](See 3.381-3). Thus, we obtain

$$I_c(w) = sgn(\sigma)\mu F_T(s) + |\sigma| \left\{ \xi^{-1}\delta_2(s) - \sum_{k=0}^{\infty} \frac{\pi^{2k}}{2^{2k}} a_k \delta_1(-2k/\xi, s) \right\},$$

where $\delta_1(v,\tau) = \int_0^\tau (1+\xi t)^v \exp(-t)dt = e^{1/\xi}\xi^v \left[\Gamma(v+1, 1/\xi) - \Gamma(v+1, \tau + 1/\xi)\right]$, and $\delta_2(\tau) = \int_0^\tau \ln(1+\xi t)\exp(-t)dt = \lim_{v\to 0} \frac{\partial}{\partial v}\delta_1(v,\tau)$.

4.3. Order Statistics

Researchers in many fields of statistics, such as reliability and life testing, have mainly used order statistics. We let $X_{(1)}, X_{(2)}, ..., X_{(n)}$ denote the ordered statistics of a random sample $X_1, X_2, \ldots, X_n$ from a continuous population with CDF $F_X(x)$ and PDF $f_X(x)$. Then, the PDF of k^{th} order statistic $X_{(k)}$ is

$$f_{X_{(k)}}(x) = k\binom{n}{k} f_X(x)[F_X(x)]^{k-1}[1 - F_X(x)]^{n-k}. \tag{4.11}$$

The PDF of the k^{th} order statistic for GHS distribution is derived by substituting (2.3) and (2.4) in (4.11). Then, using binomial theorem yields

$$f_{X_{(k)}}(x) = \binom{n}{k} \frac{2k\exp(\frac{x-\mu}{\sigma})\left(1+\exp(2\frac{x-\mu}{\sigma})\right)^{-1}}{\pi|\sigma|\left[1 - \frac{2}{\pi}\tan^{-1}\left(\exp\left(\frac{x-\mu}{\sigma}\right)\right)\right]^{\xi+1}} \sum_{j=0}^{\varpi} (-1)^j \binom{\varpi}{j} \exp\left\{ \frac{1 - \left[1 - \frac{2}{\pi}\tan^{-1}\left(\exp\left(\frac{x-\mu}{\sigma}\right)\right)\right]^{-\xi}}{(n-\varpi+j)^{-1}\xi} \right\}. \tag{4.12}$$

where $\varpi = \frac{1}{2}\left(n - 1 - sgn(\sigma)\left(n - 2k + 1\right)\right)$.

5. Estimation and simulation

5.1. Estimation

Seven estimation methods of the GHS parameters, including the maximum likelihood (ML) method, least-square and weighted least-square methods, maximum product of spacing (MPS) method, Cramér-von Mises (CVM) method, Anderson-Darling (AD) method, and method of moments (MM), are selected in this study. These methods are described in a general way to save space. Let $x_1, x_2, \ldots, x_n$ be an observed random sample of size n from the GHS distribution in (2.4), and let $x_{(1)} \le x_{(2)} \le \ldots \le x_{(n)}$ be the corresponding order statistics. Moreover, let $\theta = (\mu, \sigma, \xi)^t$ denote the vector of parameters of the GHS distribution and Θ be the parameter space. The purpose is to estimate θ by using the different methods of estimation.

5.1.1. Maximum likelihood estimators

The ML estimate for θ, as denoted by $\hat{\theta}_{ML}$, represents the values of the parameters maximizing the likelihood function or the log-likelihood function over the parameter space. The formulation is

$$\hat{\theta}_{ML} = \arg\max_{\theta\in\Theta} L_n(\theta; x_1, x_2, ..., x_n) \quad \text{or} \quad \hat{\theta}_{ML} = \arg\max_{\theta\in\Theta} \ell_n(\theta; x_1, x_2, ..., x_n),$$

where

$$L_n(\theta; x_1, x_2, ..., x_n) = \prod_{i=1}^{n} f_X(x_i|\theta) \quad \text{and} \quad \ell_n(\theta; x_1, x_2, ..., x_n) = \sum_{i=1}^{n} \ln f_X(x_i|\theta).$$

5.1.2. *Ordinary and weighted least-square estimators*

It is well-known that

$$E\left[F_X(X_{(i)}|\theta)\right] = \frac{i}{n+1} \quad \text{and} \quad \mathrm{Var}\left[F_X(X_{(i)}|\theta)\right] = \frac{i(n-i+1)}{(n+1)^2(n+2)}.$$

The ordinary least-square (OLS) estimates for θ, as denoted by $\hat{\theta}_{OLS}$, are obtained by minimizing the following sum of squares:

$$\hat{\theta}_{OLS} = \arg\min_{\theta\in\Theta} \sum_{i=1}^{n} \left[F_X(x_{(i)}|\theta) - \frac{i}{n+1}\right]^2.$$

The weighted least-square (WLS) method differs from the OLS method in terms of the weighted sum of the squared components by the inverse of their respective variances. The WLS estimate, as denoted by $\hat{\theta}_{WLS}$, is obtained from

$$\hat{\theta}_{WLS} = \arg\min_{\theta\in\Theta} \sum_{i=1}^{n} \frac{(n+1)^2(n+2)}{i(n-i+1)}\left[F_X(x_{(i)}|\theta) - \frac{i}{n+1}\right]^2.$$

5.1.3. *Maximum product of spacing estimators*

Cheng and Amin [9] and Cheng and Amin [10] introduced the MPS method as an alternative to the ML method when estimating parameters with continuous univariate distributions. The uniform spacings of a random sample from the GHS distribution is defined as

$$D_i(\theta) = F_X(x_{(i)}|\theta) - F_X(x_{(i-1)}|\theta), \; i = 1, 2, ..., n+1,$$

where $F_X(x_{(0)}|\theta) = 0$ and $F_X(x_{(n+1)}|\theta) = 1$. Thus, $\sum\limits_{i=1}^{n+1} D_i(\theta) = 1$. The MPS estimates, as denoted by $\hat{\theta}_{MPS}$, are obtained by maximizing the geometric mean of the spacings with respect to θ, that is,

$$\hat{\theta}_{MPS} = \arg\max_{\theta\in\Theta}\left[\prod_{i=1}^{n+1} D_i(\theta)\right]^{\frac{1}{n+1}} \quad \text{or} \quad \hat{\theta}_{MPS} = \arg\max_{\theta\in\Theta} \frac{1}{n+1}\sum_{i=1}^{n+1} \ln D_i(\theta).$$

5.1.4. *Cramér-von Mises estimators*

MacDonald [19] provided empirical evidence in which the bias of the CVM estimator is smaller than those of the other minimum distance estimators. The CVM estimators, as denoted by $\hat{\theta}_{CVM}$, of the parameters vector θ is obtained as

$$\hat{\theta}_{CVM} = \arg\min_{\theta\in\Theta}\left[\frac{1}{12n} + \sum_{i=1}^{n}\left(F_X(x_i|\theta) - \frac{2i-1}{2n}\right)^2\right].$$

5.1.5. Anderson-Darling estimators

The AD estimates, as denoted by $\hat{\theta}_{AD}$, are obtained by minimizing the Anderson-Darling statistic with respect to θ, that is,

$$\hat{\theta}_{AD} = \arg\min_{\theta\in\Theta} \left[-n - \sum_{i=1}^{n} \frac{2i-1}{n} \left[\ln F_X(x_{(i)}|\theta) + \ln\left(1 - F_X(x_{(n+1-i)}|\theta)\right)\right]\right].$$

5.1.6. Method of moments estimators

The MM estimates, as denoted by $\hat{\theta}_{MM}$, of the GHS distribution can be obtained by equating the first three theoretical moments of the random variable with PDF in (2.3) with the corresponding sample moments as follows:

$$E\left(X^r\right) = \frac{1}{n}\sum_{i=1}^{n} x_i^r, \; r = 1, 2, 3,$$

where $E\left(X^r\right)$ are defined in Theorem 3.3.

5.2. Simulation

In this subsection, we compare the performance of the estimation methods in previous subsection 5.1 for the parameters of the GHS distribution by conducting a simulation study. Many combinations of the parameters of the GHS model, such as highly and moderately left (or right) skewed, are considered. They represent several different possible shapes of the model. Table 2 contains the parameter sets and the corresponding central moments of the GHS distribution. The results of three sample sizes (n = 100, 200, and 500) are reported.

Table 2: Set of parameter combinations and the corresponding central moments of the GHS distribution

Parameter set			Mean	Variance	Skewness	Kurtosis
μ	σ	ξ				
-2	-1	0.5	-1.678	1.498	1.056	5.626
0	-2	1	0.984	4.848	1.428	6.856
2	-3	2	4.121	8.609	1.813	8.677
-1	1	0.5	-1.322	1.498	-1.056	5.626
0	2	1	-0.984	4.848	-1.428	6.856
4	4	2	1.172	15.305	-1.813	8.677

The methods estimators of the parameters μ, σ, and ξ are computed for 1000 repetitions to calculate the bias, $\text{Bias}(\hat{\lambda}) = \frac{1}{1000}\sum_{i=1}^{1000}(\hat{\lambda}_i - \lambda)$, and mean square error (MSE), $\text{MSE}(\hat{\lambda}) = \frac{1}{1000}\sum_{i=1}^{1000}(\hat{\lambda}_i - \lambda)^2$, $\lambda = \mu, \sigma, \xi$, and then repeated for each set of parameter combinations and sample sizes. For each parameter combination, we generate a random sample $u_i \sim \text{uniform}(0, 1)$, $i = 1, 2, ..., n$. Then $x_i = Q_X(u_i) \sim \text{GHS}(\mu, \sigma, \xi)$ distribution. The initial values of μ and σ are taken to be the mean ($\bar{x}$) and standard deviation (s) of the data, respectively. The initial value of σ is taken as s (or $-s$) if the data is skewed left (or right). The initial value of ξ is taken as 1 or 1.5. All simulations are done in R software (ver. 4.0.2). Also, the estimation processes proceed until standard convergence criteria are met.

Table 3: Simulation results

Parameters			Sample size (n)	Method	Bias			MSE			Rank Sum
μ	σ	ξ			$\hat{\mu}$	$\hat{\sigma}$	$\hat{\xi}$	$\hat{\mu}$	$\hat{\sigma}$	$\hat{\xi}$	
-2	-1	0.5	100	ML	0.034^{5}	0.012^{2}	0.079^{3}	0.031^{1}	0.024^{1}	0.106^{1}	13^{2}

Table 3 continued from previous page

Parameters			Sample size (n)	Method	Bias			MSE			Rank Sum
μ	σ	ξ			$\hat{\mu}$	$\hat{\sigma}$	$\hat{\xi}$	$\hat{\mu}$	$\hat{\sigma}$	$\hat{\xi}$	
				OLS	0.053^{7}	0.036^{7}	0.144^{7}	0.075^{5}	0.046^{6}	0.529^{5}	37^{7}
				WLS	0.031^{4}	0.020^{4}	0.079^{3}	0.043^{3}	0.031^{3}	0.188^{3}	20^{3}
				MPS	0.018^{2}	0.033^{6}	0.061^{2}	0.087^{6}	0.034^{4}	1.516^{6}	26^{4}
				CVM	0.048^{6}	0.019^{3}	0.136^{5}	0.067^{4}	0.042^{5}	0.413^{4}	27^{5}
				AD	0.021^{3}	0.009^{1}	0.052^{1}	0.035^{2}	0.027^{2}	0.127^{2}	11^{1}
				MM	0.004^{1}	0.028^{5}	0.136^{5}	0.175^{7}	0.049^{7}	4.863^{7}	32^{6}
			200	ML	0.017^{6}	0.009^{4}	0.045^{4}	0.015^{1}	0.011^{1}	0.042^{2}	18^{3}
				OLS	0.016^{5}	0.014^{6}	0.047^{5}	0.026^{6}	0.019^{6}	0.112^{6}	34^{6}
				WLS	0.012^{3}	0.010^{5}	0.034^{3}	0.018^{4}	0.013^{4}	0.062^{4}	23^{4}
				MPS	0.000^{1}	0.017^{7}	0.008^{1}	0.015^{1}	0.011^{1}	0.039^{1}	12^{1}
				CVM	0.015^{4}	0.006^{3}	0.047^{5}	0.025^{5}	0.018^{5}	0.110^{5}	27^{5}
				AD	0.008^{2}	0.005^{2}	0.027^{2}	0.017^{3}	0.012^{3}	0.052^{3}	15^{2}
				MM	0.033^{7}	0.004^{1}	0.756^{7}	0.360^{7}	0.048^{7}	233.041^{7}	36^{7}
			500	ML	0.008^{6}	0.006^{4}	0.021^{4}	0.006^{1}	0.005^{1}	0.016^{2}	18^{3}
				OLS	0.007^{4}	0.008^{6}	0.021^{4}	0.009^{5}	0.007^{5}	0.036^{5}	29^{6}
				WLS	0.005^{3}	0.006^{4}	0.016^{3}	0.007^{3}	0.005^{1}	0.022^{4}	18^{3}
				MPS	0.002^{1}	0.008^{6}	0.001^{1}	0.006^{1}	0.005^{1}	0.015^{1}	11^{1}
				CVM	0.007^{4}	0.005^{3}	0.021^{4}	0.009^{5}	0.007^{5}	0.036^{5}	26^{5}
				AD	0.004^{2}	0.004^{2}	0.013^{2}	0.007^{3}	0.005^{1}	0.021^{3}	13^{2}
				MM	0.021^{7}	0.002^{1}	0.613^{7}	0.134^{7}	0.019^{7}	222.761^{7}	36^{7}
0	-2	1	100	ML	0.161^{3}	0.062^{3}	0.357^{2}	0.736^{2}	0.174^{2}	7.654^{5}	17^{2}
				OLS	0.275^{7}	0.137^{7}	0.564^{5}	1.139^{5}	0.345^{6}	4.856^{4}	34^{7}
				WLS	0.196^{5}	0.097^{5}	0.410^{3}	0.865^{3}	0.252^{3}	4.063^{3}	22^{3}
				MPS	0.190^{4}	0.135^{6}	0.568^{6}	1.731^{6}	0.281^{4}	32.303^{6}	32^{6}
				CVM	0.228^{6}	0.089^{4}	0.477^{4}	0.895^{4}	0.292^{5}	3.478^{2}	25^{4}
				AD	0.115^{2}	0.053^{2}	0.222^{1}	0.431^{1}	0.173^{1}	1.296^{1}	8^{1}
				MM	0.099^{1}	0.035^{1}	1.207^{7}	4.591^{7}	0.429^{7}	380.586^{7}	30^{5}
			200	ML	0.055^{4}	0.025^{3}	0.092^{4}	0.098^{1}	0.057^{1}	0.159^{2}	15^{2}
				OLS	0.081^{6}	0.047^{6}	0.149^{6}	0.252^{6}	0.118^{6}	0.674^{5}	35^{6}
				WLS	0.052^{3}	0.031^{5}	0.091^{3}	0.139^{4}	0.077^{4}	0.270^{4}	23^{4}
				MPS	0.028^{1}	0.050^{7}	0.049^{1}	0.099^{2}	0.064^{2}	0.155^{1}	14^{1}
				CVM	0.072^{5}	0.027^{4}	0.141^{5}	0.243^{5}	0.112^{5}	0.683^{6}	30^{5}
				AD	0.039^{2}	0.020^{2}	0.071^{2}	0.118^{3}	0.069^{3}	0.202^{3}	15^{2}
				MM	0.123^{7}	0.006^{1}	1.290^{7}	4.725^{7}	0.337^{7}	432.197^{7}	36^{7}
			500	ML	0.025^{4}	0.015^{3}	0.041^{4}	0.037^{1}	0.024^{1}	0.056^{2}	15^{2}
				OLS	0.033^{6}	0.024^{7}	0.056^{6}	0.071^{6}	0.043^{6}	0.132^{6}	37^{7}
				WLS	0.022^{3}	0.017^{4}	0.038^{3}	0.047^{4}	0.030^{4}	0.077^{4}	22^{4}
				MPS	0.006^{1}	0.022^{6}	0.014^{1}	0.037^{1}	0.025^{2}	0.054^{1}	12^{1}
				CVM	0.030^{5}	0.017^{4}	0.053^{5}	0.070^{5}	0.042^{5}	0.130^{5}	29^{5}
				AD	0.018^{2}	0.013^{2}	0.033^{2}	0.045^{3}	0.029^{3}	0.073^{3}	15^{2}
				MM	0.067^{7}	0.006^{1}	0.556^{7}	1.678^{7}	0.133^{7}	176.303^{7}	36^{6}
2	-3	2	100	ML	0.556^{2}	0.163^{2}	1.347^{3}	4.903^{3}	0.71^{1}	47.066^{5}	16^{2}
				OLS	0.834^{6}	0.315^{6}	1.633^{6}	5.396^{5}	1.129^{6}	18.781^{3}	32^{6}
				WLS	0.722^{5}	0.264^{5}	1.478^{5}	5.009^{4}	0.953^{3}	19.851^{4}	26^{5}
				MPS	1.287^{7}	0.482^{7}	3.566^{7}	17.341^{7}	1.912^{7}	187.114^{7}	42^{7}
				CVM	0.686^{4}	0.219^{4}	1.396^{4}	4.478^{2}	0.965^{4}	15.280^{1}	19^{3}
				AD	0.575^{3}	0.198^{3}	1.184^{2}	4.113^{1}	0.811^{2}	16.330^{2}	13^{1}
				MM	0.022^{1}	0.101^{1}	0.750^{1}	6.820^{6}	0.985^{5}	50.662^{6}	20^{4}
			200	ML	0.225^{3}	0.075^{2}	0.450^{2}	1.323^{2}	0.268^{1}	8.630^{5}	15^{2}
				OLS	0.399^{7}	0.157^{6}	0.733^{5}	2.265^{5}	0.544^{6}	6.664^{4}	33^{6}
				WLS	0.272^{4}	0.109^{4}	0.485^{3}	1.384^{3}	0.361^{3}	3.836^{2}	19^{3}
				MPS	0.391^{6}	0.187^{7}	0.942^{6}	3.928^{6}	0.531^{5}	36.947^{6}	36^{7}
				CVM	0.335^{5}	0.111^{5}	0.633^{4}	1.956^{4}	0.491^{4}	5.489^{3}	25^{4}
				AD	0.210^{2}	0.081^{3}	0.367^{1}	1.029^{1}	0.306^{2}	2.304^{1}	10^{1}
				MM	0.144^{1}	0.033^{1}	1.149^{7}	8.883^{7}	0.803^{7}	221.641^{7}	30^{5}
			500	ML	0.084^{2}	0.036^{2}	0.130^{2}	0.225^{1}	0.088^{1}	0.376^{1}	9^{1}
				OLS	0.171^{7}	0.079^{7}	0.276^{6}	0.651^{6}	0.204^{6}	1.366^{6}	38^{7}
				WLS	0.102^{4}	0.049^{4}	0.160^{4}	0.340^{4}	0.122^{4}	0.618^{4}	24^{4}
				MPS	0.074^{1}	0.061^{5}	0.107^{1}	0.245^{2}	0.098^{2}	0.403^{2}	13^{2}
				CVM	0.154^{6}	0.063^{6}	0.257^{5}	0.621^{5}	0.196^{5}	1.301^{5}	32^{5}
				AD	0.089^{3}	0.041^{3}	0.142^{3}	0.317^{3}	0.118^{3}	0.561^{3}	18^{3}
				MM	0.133^{5}	0.008^{1}	0.707^{7}	3.695^{7}	0.366^{7}	73.579^{7}	34^{6}
-1	1	0.5	100	ML	0.034^{5}	0.012^{2}	0.079^{3}	0.031^{1}	0.024^{1}	0.106^{1}	13^{2}
				OLS	0.053^{7}	0.036^{7}	0.144^{7}	0.075^{5}	0.046^{6}	0.529^{5}	37^{7}
				WLS	0.031^{4}	0.020^{4}	0.079^{3}	0.043^{3}	0.031^{3}	0.188^{3}	20^{3}
				MPS	0.018^{2}	0.033^{6}	0.061^{2}	0.087^{6}	0.034^{4}	1.516^{6}	26^{4}
				CVM	0.048^{6}	0.019^{3}	0.136^{5}	0.067^{4}	0.042^{5}	0.413^{4}	27^{5}
				AD	0.021^{3}	0.009^{1}	0.052^{1}	0.035^{2}	0.027^{2}	0.127^{2}	11^{1}
				MM	0.004^{1}	0.028^{5}	0.136^{5}	0.175^{7}	0.049^{7}	4.863^{7}	32^{6}

Table 3 continued from previous page

Parameters			Sample size	Method	Bias			MSE			Rank
μ	σ	ξ	(n)		$\hat{\mu}$	$\hat{\sigma}$	$\hat{\xi}$	$\hat{\mu}$	$\hat{\sigma}$	$\hat{\xi}$	Sum
			200	ML	0.019^{5}	0.008^{2}	0.043^{4}	0.016^{2}	0.013^{1}	0.048^{2}	16^{3}
				OLS	0.026^{7}	0.019^{7}	0.065^{5}	0.026^{5}	0.021^{6}	0.120^{6}	36^{7}
				WLS	0.016^{3}	0.010^{4}	0.037^{3}	0.018^{4}	0.015^{4}	0.064^{4}	22^{4}
				MPS	0.003^{1}	0.016^{6}	0.007^{1}	0.015^{1}	0.013^{1}	0.045^{1}	11^{1}
				CVM	0.025^{6}	0.011^{5}	0.065^{5}	0.026^{5}	0.020^{5}	0.116^{5}	31^{5}
				AD	0.012^{2}	0.006^{1}	0.029^{2}	0.017^{3}	0.014^{3}	0.055^{3}	14^{2}
				MM	0.016^{3}	0.009^{3}	0.107^{7}	0.098^{7}	0.032^{7}	1.348^{7}	34^{6}
			500	ML	0.008^{5}	0.004^{2}	0.016^{4}	0.006^{1}	0.004^{1}	0.015^{2}	15^{3}
				OLS	0.011^{7}	0.008^{7}	0.024^{5}	0.010^{5}	0.007^{5}	0.037^{5}	34^{7}
				WLS	0.007^{4}	0.005^{4}	0.015^{3}	0.007^{3}	0.005^{3}	0.021^{4}	21^{4}
				MPS	0.002^{1}	0.006^{6}	0.005^{1}	0.006^{1}	0.004^{1}	0.014^{1}	11^{1}
				CVM	0.010^{6}	0.005^{4}	0.025^{6}	0.010^{5}	0.007^{5}	0.037^{5}	31^{5}
				AD	0.006^{2}	0.003^{1}	0.012^{2}	0.007^{3}	0.005^{3}	0.020^{3}	14^{2}
				MM	0.006^{2}	0.004^{2}	0.032^{7}	0.028^{7}	0.012^{7}	0.149^{7}	32^{6}
0	2	1	100	ML	0.124^{4}	0.038^{2}	0.247^{2}	0.506^{2}	0.155^{1}	4.319^{4}	15^{2}
				OLS	0.262^{7}	0.127^{7}	0.520^{6}	1.045^{6}	0.339^{7}	4.536^{5}	38^{7}
				WLS	0.169^{5}	0.079^{4}	0.341^{4}	0.709^{3}	0.233^{4}	3.551^{3}	23^{3}
				MPS	0.116^{3}	0.100^{6}	0.248^{3}	0.763^{4}	0.211^{3}	6.265^{6}	25^{4}
				CVM	0.221^{6}	0.082^{5}	0.448^{5}	0.851^{5}	0.294^{5}	3.408^{2}	28^{5}
				AD	0.093^{2}	0.037^{1}	0.162^{1}	0.314^{1}	0.165^{2}	0.744^{1}	8^{1}
				MM	0.019^{1}	0.071^{3}	0.715^{7}	2.538^{7}	0.316^{6}	148.042^{7}	31^{6}
			200	ML	0.061^{4}	0.023^{3}	0.094^{3}	0.112^{1}	0.070^{1}	0.205^{1}	13^{1}
				OLS	0.109^{7}	0.061^{7}	0.185^{6}	0.276^{6}	0.132^{6}	0.756^{6}	38^{7}
				WLS	0.062^{5}	0.033^{4}	0.100^{4}	0.147^{4}	0.085^{4}	0.292^{4}	25^{4}
				MPS	0.037^{1}	0.049^{6}	0.056^{1}	0.124^{2}	0.079^{2}	0.235^{2}	14^{2}
				CVM	0.099^{6}	0.041^{5}	0.173^{5}	0.257^{5}	0.125^{5}	0.689^{5}	31^{5}
				AD	0.049^{2}	0.022^{1}	0.08^{2}	0.134^{3}	0.081^{3}	0.255^{3}	14^{2}
				MM	0.054^{3}	0.022^{1}	0.366^{7}	1.139^{7}	0.200^{7}	15.650^{7}	32^{6}
			500	ML	0.024^{4}	0.010^{1}	0.034^{3}	0.035^{2}	0.023^{1}	0.052^{2}	13^{2}
				OLS	0.040^{7}	0.025^{7}	0.063^{6}	0.073^{6}	0.042^{5}	0.139^{6}	37^{7}
				WLS	0.025^{5}	0.014^{4}	0.037^{4}	0.045^{4}	0.028^{3}	0.073^{4}	24^{4}
				MPS	0.005^{1}	0.017^{5}	0.006^{1}	0.034^{1}	0.024^{2}	0.050^{1}	11^{1}
				CVM	0.037^{6}	0.017^{5}	0.060^{5}	0.071^{5}	0.042^{5}	0.137^{5}	31^{5}
				AD	0.020^{3}	0.010^{1}	0.030^{2}	0.043^{3}	0.028^{3}	0.069^{3}	15^{3}
				MM	0.019^{2}	0.011^{3}	0.102^{7}	0.282^{7}	0.075^{7}	1.117^{7}	33^{6}
4	4	2	100	ML	0.616^{2}	0.158^{1}	1.070^{1}	6.973^{1}	1.155^{1}	33.747^{5}	11^{1}
				OLS	1.068^{6}	0.397^{6}	1.521^{5}	9.170^{5}	2.025^{5}	17.024^{3}	30^{5}
				WLS	0.915^{5}	0.324^{5}	1.367^{4}	8.663^{4}	1.748^{3}	18.759^{4}	25^{4}
				MPS	1.550^{7}	0.567^{7}	3.277^{6}	28.337^{6}	3.159^{7}	175.497^{6}	39^{7}
				CVM	0.902^{4}	0.277^{3}	1.348^{3}	7.972^{3}	1.780^{4}	15.185^{1}	18^{3}
				AD	0.712^{3}	0.229^{2}	1.076^{2}	7.123^{2}	1.499^{2}	15.641^{2}	13^{2}
				MM	0.147^{1}	0.300^{4}	38.248^{7}	41.989^{7}	2.783^{6}	1138692.451^{7}	32^{6}
			200	ML	0.338^{2}	0.100^{1}	0.507^{2}	3.102^{2}	0.607^{1}	10.430^{5}	13^{2}
				OLS	0.615^{7}	0.250^{6}	0.798^{5}	3.970^{5}	1.022^{5}	6.134^{4}	32^{5}
				WLS	0.436^{4}	0.166^{3}	0.600^{3}	3.191^{3}	0.757^{3}	6.047^{3}	19^{3}
				MPS	0.605^{6}	0.260^{7}	1.139^{6}	9.416^{6}	1.194^{6}	51.943^{6}	37^{7}
				CVM	0.526^{5}	0.187^{4}	0.699^{4}	3.476^{4}	0.924^{4}	5.236^{2}	23^{4}
				AD	0.341^{3}	0.122^{2}	0.454^{1}	2.488^{1}	0.668^{2}	3.994^{1}	10^{1}
				MM	0.071^{1}	0.197^{5}	47.237^{7}	41.952^{7}	2.489^{7}	1040813.433^{7}	34^{6}
			500	ML	0.100^{2}	0.034^{1}	0.112^{2}	0.376^{1}	0.150^{1}	0.353^{1}	8^{1}
				OLS	0.253^{7}	0.110^{6}	0.307^{6}	1.256^{6}	0.368^{6}	1.610^{6}	37^{6}
				WLS	0.134^{5}	0.058^{3}	0.153^{4}	0.567^{4}	0.204^{4}	0.580^{4}	24^{4}
				MPS	0.086^{1}	0.067^{4}	0.089^{1}	0.413^{2}	0.167^{2}	0.387^{2}	12^{2}
				CVM	0.228^{6}	0.088^{5}	0.283^{5}	1.175^{5}	0.351^{5}	1.486^{5}	31^{5}
				AD	0.118^{4}	0.048^{2}	0.137^{3}	0.550^{3}	0.200^{3}	0.564^{3}	18^{3}
				MM	0.100^{2}	0.120^{7}	0.436^{7}	5.121^{7}	0.853^{7}	21.334^{7}	37^{6}

Table 4: Overall performance of the estimation methods

Parameters			Sample size	Method						
μ	σ	ξ	n	ML	OLS	WLS	MPS	CVM	AD	MM
-2	-1	0.5	100	2	7	3	4	5	1	6
			200	3	6	4	1	5	2	7
			500	3	6	3	1	5	2	7
			Total	8	19	10	6	15	5	20
0	-2	1	100	2	7	3	6	4	1	5
			200	2	6	4	1	5	2	7
			500	2	7	4	1	5	2	6
			Total	6	20	11	8	14	5	18
2	-3	2	100	2	6	5	7	3	1	4
			200	2	6	3	7	4	1	5
			500	1	7	4	2	5	3	6
			Total	5	19	12	16	12	5	15
-1	1	0.5	100	2	7	3	4	5	1	6
			200	3	7	4	1	5	2	6
			500	3	7	4	1	5	2	6
			Total	8	21	11	6	15	5	18
0	2	1	100	2	7	3	4	5	1	6
			200	1	7	4	2	5	2	6
			500	2	7	4	1	5	3	6
			Total	5	21	11	7	15	6	18
4	4	2	100	1	5	4	7	3	2	6
			200	2	5	3	7	4	1	6
			500	1	6	4	2	5	3	6
			Total	4	16	11	16	12	6	18
			Overall total	36^{2}	116^{7}	66^{4}	59^{3}	83^{5}	32^{1}	107^{6}

The performances of the various estimators in terms of biases and MSEs are summarized in Table 3. The column that indicates rank sum gives the partial sum of the ranks. For each estimator a superscript is used to show the rank of that estimator among the other estimators for that metric. For example, Table 3 presents the bias of the ML ($\hat{\mu}$) as 0.034^5 for $n = 100$. This shows that the bias of $\hat{\mu}$ calculated using the method of ML ranks 5^{th} among all other estimators. Table 4 displays the partial and overall rank of the estimators. This technique was used previously in Dey et al. [12] and Tahir et al. [25]. Using the results in Tables 3 and 4, we observe that the MSE values for the estimates using MM are worse (higher) than the results obtained using the other methods, while the MSE values for the estimates by ML are, in general, better (smaller) than the results obtained using the other methods. Furthermore, under all methods, except the MM method, the absolute bias and MSE values for the estimates decrease as sample size increases. As seen in Table 4, the AD method is considered as the best method among methods discussed in the paper to estimate the GHS parameters (overall score of 32). We further notice that ML method is the second most effective estimator with an overall score of 36.

6. Applications

We apply the GHS distribution to fit two data. Between the two data sets, the first data set consists of fracture toughness from the silicon nitride. The data taken from the website *https://goo.gl/UMx3h9* were already studied by Nadarajah and Kotz [22] and Cordeiro et al. [11]. The second data set contains the breaking times (in hour) for Kevlar 49/Epoxy strands that were studied in stress of 373.9 Ksi and a temperature of 110°C. These data were reported by Glaser [16]. The descriptive statistics of the two data sets are shown in Table 5.

Table 5: The summary statistics of the data sets.

Data set	No. of Obs.	Mean	Std. Dev.	Skewness	Kurtosis
The Alumina (Al2O3)	119	4.3254	1.0185	-0.4167	3.0935
The Kevlar-49/epoxy	76	1.9592	1.574	1.9796	8.1608

The shape of an HRF decides whether a particular distribution is suitable for a data set. The empirical behavior of the HRF can be obtained using the total time on test (TTT) plot of the data. It can also be utilized to choose a suitable model for describing the data set. Additional details can be found in Aarset [1]. Figures 5(a) and 5(b) display the plot for the two data sets, respectively. The TTT plot for the first data in Figure 5(a) indicates an increasing HRF, while the TTT plot for the second data in Figure 5(b) indicates an S-shaped (constant - increase - constant) HRF. Therefore, the appropriateness of the GHS distribution to fit the data sets is demonstrated by the plots. Specifically, the new model can present increasing and S-shaped HRF.

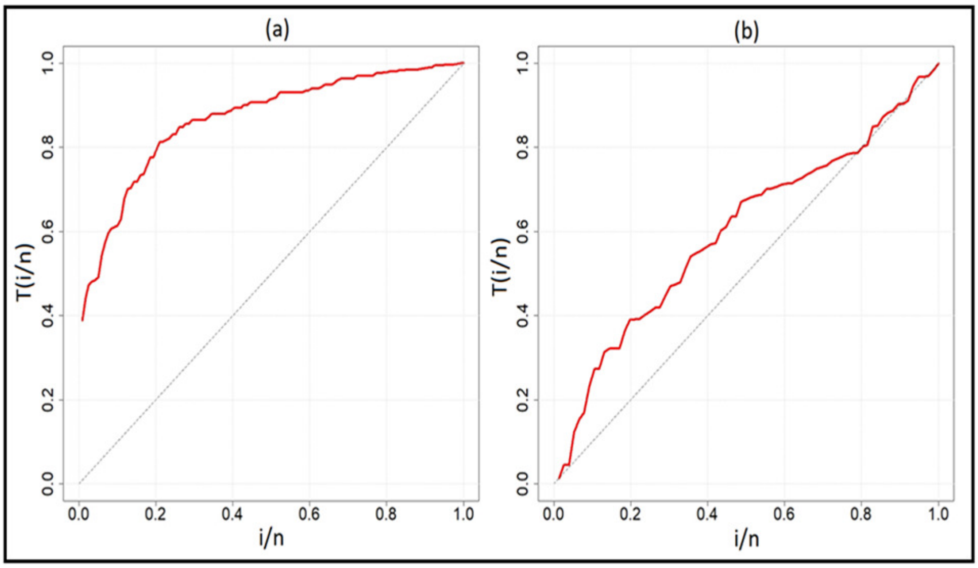

Figure 5: TTT plot: (a) The Alumina (Al2O3) data set. (b) The Kevlar-49/epoxy data set.

Comparison of the fits of the GHS distribution with those of other generalizations of HS and other distributions is conducted. The comparison models are as follows: The HS-SAS distribution by Fischer and Herrmann [14], the BHS distribution by Fischer and Vaughan [15], the BVIII distribution by Burr [8], the GLI and GLII distributions by Johnson et al. [18], and the SN distribution by Azzalini [7]. The densities of the compared distributions are defined as follows:
- HS-SAS distribution:

$$f_{HS-SAS}(x;\mu,\sigma,\delta,\varepsilon)=\frac{\cosh\left(\delta\sinh^{-1}\left(\frac{x-\mu}{\sigma}\right)-\varepsilon\right)\delta e^{\sinh\left(\delta\sinh^{-1}\left(\frac{x-\mu}{\sigma}\right)-\varepsilon\right)}}{\frac{\pi}{2}\sqrt{1+x^2}\left(1+\left(e^{\sinh\left(\delta\sinh^{-1}\left(\frac{x-\mu}{\sigma}\right)-\varepsilon\right)}\right)^2\right)},\ -\infty<\mu,\delta,\varepsilon,x<\infty,\ \sigma>0.$$

- BHS distribution:

$$f_{BHS}(x;\mu,\sigma,\beta_1,\beta_2)=\frac{B(\beta_1,\beta_2)^{-1}}{\pi\sigma\cosh\left(\frac{x-\mu}{\sigma}\right)}\frac{\left[\frac{2}{\pi}tan^{-1}\left(\exp\left(\frac{x-\mu}{\sigma}\right)\right)\right]^{\beta_1-1}}{\left[1-\frac{2}{\pi}tan^{-1}\left(\exp\left(\frac{x-\mu}{\sigma}\right)\right)\right]^{1-\beta_2}},-\infty<x,\mu<\infty,\beta_1,\beta_2,\sigma>0,$$

where $B(a,b)$ is the beta function.
- BVIII distribution:

$$f_{BVIII}(x;\mu,\sigma,r)=\frac{r}{\pi\sigma}sech\left(\frac{x-\mu}{\sigma}\right)\left(\frac{2}{\pi}tan^{-1}\left(\exp\left(\frac{x-\mu}{\sigma}\right)\right)\right)^{r-1},-\infty<x,\mu<\infty,r,\sigma>0.$$

- GLI distribution:

$$f_{GLI}(x;\mu,\sigma,\alpha)=\frac{\alpha e^{-\left(\frac{x-\mu}{\sigma}\right)}}{\left(1+e^{-\left(\frac{x-\mu}{\sigma}\right)}\right)^{\alpha+1}},\ -\infty<x,\mu<\infty,\ \sigma,\alpha>0.$$

- GLII distribution:

$$f_{GLII}(x;\mu,\sigma,\alpha)=\frac{\alpha e^{-\alpha\left(\frac{x-\mu}{\sigma}\right)}}{\left(1+e^{-\left(\frac{x-\mu}{\sigma}\right)}\right)^{\alpha+1}},\ -\infty<x,\mu<\infty,\ \sigma,\alpha>0.$$

- SN distribution:

$$f_{SN}(x;\mu,\sigma,\lambda)=\frac{2}{\sigma}\phi\left(\frac{x-\mu}{\sigma}\right)\Phi\left(\lambda\left(\frac{x-\mu}{\sigma}\right)\right),-\infty<x,\mu,\lambda<\infty,\sigma>0.$$

The model parameters in these applications are estimated using maximum likelihood method. The Akaike information criterion (AIC) and Kolmogorov-Smirnov (KS) statistic and its p-value are used to compare the fitted distributions. Small values of AIC and KS and a large p-value of KS correspond to a good fit of data. We demonstrate the plots of the fitted PDFs of some models for visual comparison.

6.1. Alumina (Al2O3) Data

The Alumina (Al2O3) data set is fitted to the GHS model presented in Section 2 and HS-SAS, BHS, BVIII, GLI, GLII, and SN distributions. As shown in Table 6, the p-values of KS statistics of the distributions provide adequate fit to the data. However, GHS provides the best fit to the data set among the other models. Therefore, the GHS distribution is a better alternate distribution to BVII, BHS, HS-SAS, GLI, GLII, and SN distributions. The GHS distribution has small AIC and KS values. Thus, it is an appropriate model to describe the alumina data. Some estimated PDFs of the fitted distributions are shown in Figure 6(a). Reasonable fits to the data set are observed for GHS, GLI, and GLII distributions. Figure 6(b) presents QQ plots with simulated envelopes for the GHS distribution. As observed, all observations fall inside the envelope of the GHS model. The observations approximately lie on a straight diagonal line as well. Therefore, the GHS model presents an outstanding fit to the data.

6.2. Kevlar-49/epoxy Data

For the Kevlar-49/epoxy data set, we fit GHS, BHS, HS-SAS, BVIII, GLI, GLII, and SN models. As shown in Table 7, a better fit to the data set is observed for GHS than the other distributions. The reason is that GHS has the smallest KS value among others. However, all models show adequate fit to the data set according to the p-values of the KS test statistics. Figure 7(a) presents plots of estimated PDFs to the Kevlar-49/epoxy data set. Evidently, the models provide an adequate fit to the data. QQ plots with simulated envelopes for the GHS distribution are shown in Figure 7(b). Notably, no observations fall outside the envelope, and they fall approximately in a straight line. Therefore, the GHS model represents the data properly as observed from the plot.

Table 6: MLEs, their standard errors (SEs) (in parentheses) and goodness of fit measures for the Alumina (Al2O3) data set.

Distribution	MLE				AIC	K-S	P-value
GHS(μ, σ, ξ)	4.494 (0.110)	0.790 (0.099)	0.282 (0.166)		343.218	0.042	0.984
HS-SAS($\mu, \sigma, \delta, \varepsilon$)	4.663 (0.195)	0.917 (0.288)	1.256 (0.268)	-0.329 (0.198)	345.157	0.050	0.918
BHS($\mu, \sigma, \beta_1, \beta_2$)	5.275 (1.168)	1.294 (1.106)	2.064 (2.714)	4.362 (7.598)	345.127	0.052	0.910
BVIII(μ, σ, r)	4.696 (0.194)	0.557 (0.083)	0.666 (0.170)		344.789	0.050	0.922
GLI(μ, σ, α)	4.811 (0.212)	0.440 (0.071)	0.564 (0.166)		343.236	0.045	0.971
GLII(μ, σ, α)	5.104 (0.502)	0.691 (0.088)	2.210 (1.103)		343.605	0.049	0.938
SN(μ, σ, λ)	4.310 (1.773)	1.014 (0.071)	0.018 (2.188)		347.065	0.088	0.310

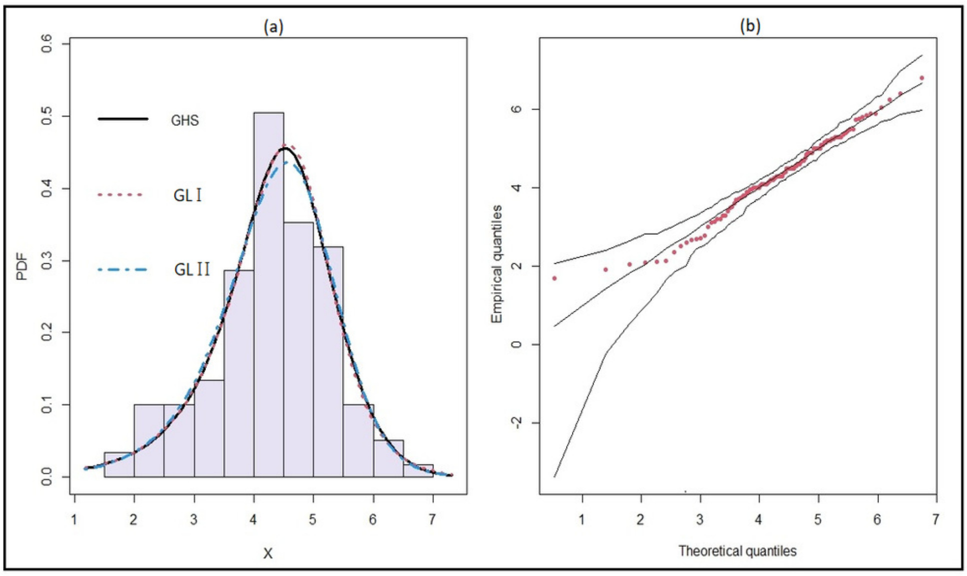

Figure 6: The Alumina data set: (a) Fitted GHS, GLI and GLII PDFs. (b) The QQ plots with simulated envelopes based on GHS.

Table 7: MLEs, their SEs (in parentheses) and goodness of fit measures for the Kevlar-49/epoxy data set.

Distribution	MLE				AIC	K-S	P-value
GHS(μ, σ, ξ)	0.461 (0.959)	-1.724 (0.535)	3.140 (2.695)		248.907	0.075	0.752
HS-SAS(μ, σ, δ, ε)	0.786 (0.312)	0.716 (0.194)	1.083 (0.210)	1.000 (0.396)	253.635	0.084	0.632
BHS(μ, σ, β_1, β_2)	-0.593 (0.940)	0.492 (0.185)	14.735 (28.376)	0.352 (0.174)	251.585	0.086	0.603
BVIII(μ, σ, r)	-0.785 (1.339)	1.030 (0.099)	11.658 (16.081)		253.894	0.090	0.532
GLI(μ, σ, α)	-3.085 (2.246)	0.999 (0.094)	83.417 (179.348)		254.750	0.092	0.516
GLII(μ, σ, α)	0.554 (0.173)	0.237 (0.079)	0.163 (0.068)		250.856	0.082	0.662
SN(μ, σ, λ)	0.172 (0.168)	2.374 (0.230)	10.878 (8.562)		257.132	0.148	0.064

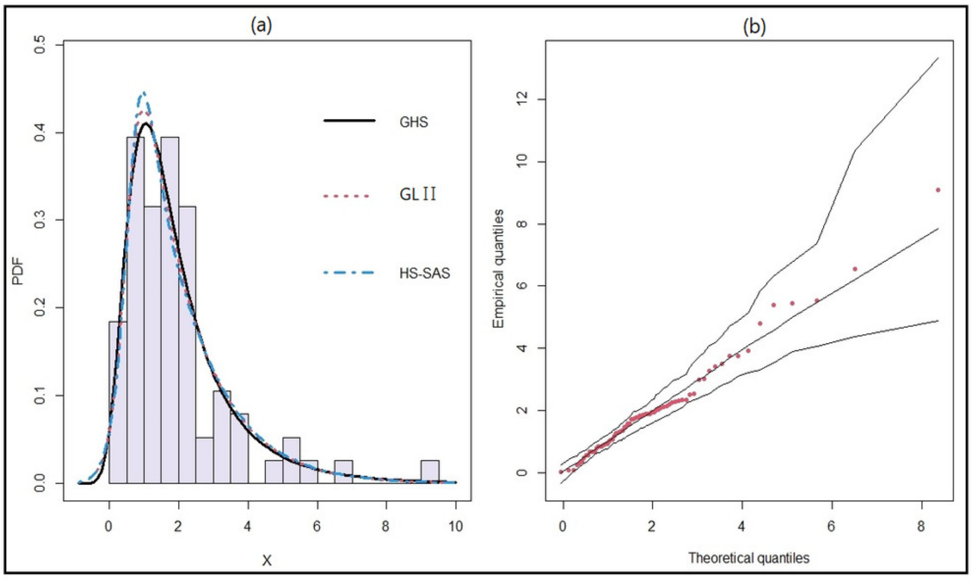

Figure 7: The Kevlar-49/epoxy data set: (a) Fitted GHS, GLII and HS-SAS PDFs. (b) The QQ plots with simulated envelopes based on GHS.

The various estimation methods examined in Section 5 are utilized to estimate the unknown parameters. Tables 8 and 9 show the estimates of the unknown parameters obtained using the seven methods and the K-S values for first and second data set, respectively. The tables show that although most of the methods performed well, the CVM method is recommended for estimating the parameters of the GHS distribution for first and second data set.

Table 8: The parameter estimates under various methods and the goodness of fit statistics for Alumina (Al2O3) data set.

Method	Parameters			$-\ell$	K-S	p-value
	$\hat{\mu}$	$\hat{\sigma}$	$\hat{\xi}$			
ML	4.4940	0.7898	0.2815	168.6089	0.0423	0.9837
OLS	4.4860	0.7956	0.2587	168.6566	0.0440	0.9753
WLS	4.4924	0.8074	0.2775	168.6610	0.0453	0.9676
MPS	4.2871	1.0225	0.2136	175.9975	0.1458	0.0127
CVM	4.4848	0.7840	0.2571	168.6246	0.0418	0.9854
AD	4.5042	0.8150	0.3127	168.6405	0.0446	0.9722
MM	4.3971	0.7053	0.1105	169.3565	0.0622	0.7470

Table 9: The parameter estimates under various methods and the goodness of fit statistics for Kevlar-49/epoxy data set

Method	Parameter estimates			$-\ell$	K-S	p-value
	$\hat{\mu}$	$\hat{\sigma}$	$\hat{\xi}$			
ML	0.4611	-1.7242	3.1404	121.4533	0.0754	0.7517
OLS	1.1739	-1.2696	1.2196	122.4967	0.0674	0.8574
WLS	0.8345	-1.5174	2.0797	121.6388	0.0742	0.7692
MPS	0.0724	-1.9947	4.1178	121.6821	0.0885	0.5605
CVM	1.2053	-1.2261	1.1565	122.6199	0.0649	0.8850
AD	0.7725	-1.5459	2.2738	121.5450	0.0735	0.7783
MM	0.5840	-1.6879	2.7020	121.5772	0.0787	0.7038

7. Summary and Conclusions

In this study, a new generalization for the HS distribution, which is called the GHS distribution, is proposed. The structural properties of this new distribution are studied. The relationships between the parameters and the mean, variance, skewness, and kurtosis are also explored. The GHS distribution can fit data with a very wide range of skewness (left and right) and kurtosis with only three parameters. Different estimation techniques can estimate the unknown parameters of a new distribution. Here, simulation is performed to identify the best performing estimators among a set of selected methods. The simulation results indicate that the AD estimators are the best performing estimators for the biases and MSEs when estimating the parameters of the GHS distribution. The usefulness of the new distribution for fitting skewed data is demonstrated using two real data sets. The proposed GHS can fit highly skewed data sets effectively as suggested by the applications.

Acknowledgments

The author is very grateful to the handling Editor and the anonymous reviewers for valuable comments and suggestions for improved the paper.

References

[1] M. V. Aarset, How to identify bathtub hazard rate, IEEE Trans Reliab, 36 (1987) 106-108.
[2] M. Abramowitz, I. A. Stegun, Handbook of Mathematical Functions with Formulas, Graphs, and Mathematical Tables, Dover, New York, (1972).
[3] M. A. Aljarrah, F. Famoye, C. Lee, A new generalized normal distribution: Properties and applications, Communications in Statistics - Theory and Methods, 48(18), (2019) 4474-4491.
[4] M. A. Aljarrah, C. Lee, F. Famoye, On generating *T-X* family of distributions using quantile functions, Journal of Statistical Distribution and Application, 1 (2014) Article No. 2.
[5] A. Alzaatreh, C. Lee, F. Famoye, A new method for generating families of continuous distributions, Metron, 71 (2013) 63-79.
[6] D. F. Andrews, A. M. Herzberg, Data: A Collection of Problems from Many Fields for the Student and Research Worker, Springer Series in Statistics, New York, (1985).
[7] A. Azzalini, A class of distributions which includes the normal ones, Scandinavian Journal of Statistics, 12 (1985) 171-178.
[8] I. W. Burr, Cumulative Frequency Functions, The Annals of Mathematical Statistics, 13 (1942) 215-232.
[9] R. C. H. Cheng, N. A. K. Amin, Maximum product-of-spacings estimation with applications to the lognormal distribution, University of Wales IST, Math Report79-1, (1979).
[10] R. C. H. Cheng, N. A. K. Amin, Estimating parameters in continuous univariate distributions with a shifted origin, Journal of the Royal Statistical Society; Series B, 45 (1983) 394-403.
[11] G. M. Cordeiro, M. Alizadeh, R. B. Silva, T. G. Ramires, A new wider family of continuous models: the extended Cordeiro and de Castro family, Hacettepe Journal of Mathematics and Statistics, 47(4), (2018) 937-961.
[12] S. Dey, E. Raheem, S. Mukherjee, Statistical properties and different methods of estimation of transmuted Rayleigh distribution, Revista Colombiana de Estadística, 40(1), (2017) 165-203.
[13] M. J. Fischer, Generalized hyperbolic secant distribution-with application to finance, Springer, Berlin, (2014).
[14] M. Fischer, K. Herrmann, The HS-SAS and GSH-SAS distribution as model for unconditional and conditional return distributions, Austrian Journal of Statistics, 42 (2013) 33-45.
[15] M. Fischer, D. C. Vaughan, The Beta-hyperbolic secant (BHS) distribution, Austrian Journal of Statistics, 39(2), (2010) 245-258.
[16] R. E. Glaser, Statistical Analysis of Kevlar 49/Epoxy Composite Stress-Rupture Data, Report UCID-19849, Lawrence Livermore National Laboratory, Livermore, CA, (1983).
[17] I. S. Gradshteyn, I. M. Ryzhik, Table of Integrals, Series, and Products, Academic Press, New York, (2000).
[18] N. L. Johnson, S. Kotz, N. Balakrishnan, Continuous Univariate Distributions: Vol. 2, (2nd Edition), John Wiley and Sons, New York, (1995).
[19] P. D. M. MacDonald, Comment on 'An Estimation Procedure for Mixtures of Distributions' by Choi and Bulgren, Journal of the Royal Statistical Society; Series B, 33 (1971) 326-329.
[20] M. S. Milgram, The generalized integro-exponential function, Mathematics of Computation, 44(170), (1985) 443-458.
[21] G. S. Mudholkar, D. K. Srivastava, G. D. Kollia, A generalization of the Weibull distribution with application to the analysis of survival data, Journal of the American Statistical Association, 91 (1996) 1575-1583.
[22] S. Nadarajah, S. Kotz, On the alternative to the Weibull function, Engineering Fracture Mechanics, 74(3), (2007) 451-456.
[23] W. F. Perks, On some experiments in the graduation of mortality statistics, Journal of the Institute of Actuaries, 58 (1932) 12-57.
[24] C. E. Shannon, A mathematical theory of communication, Bell System Technical Journal, 27 (1948) 379-432.
[25] M. Tahir, G. M. Cordeiro, S. Ali, S. Dey, A. Manzoor, The inverted Nadarajah-Haghighi distribution: estimation methods and applications, Journal of Statistical Computation and Simulation, 88(14), (2018) 2775-2798.
[26] J. Talacko, Perks' distributions and their role in the theory of Wiener's stochastic variables, Trabajos de Estadistica, 7 (1956) 159-174.